

RAL-TR-95-078
20 December 1995

No Mikheyev-Smirnov-Wolfenstein Effect in Maximal Mixing

P. F. Harrison

Physics Department, Queen Mary and Westfield College
Mile End Rd. London E1 4NS. UK ¹

and

D. H. Perkins

Nuclear Physics Laboratory, University of Oxford
Keble Road, Oxford OX1 3RH. UK ²

and

W. G. Scott

Rutherford Appleton Laboratory
Chilton, Didcot, Oxon OX11 0QX. UK ³

Abstract

We investigate the possible influence of the MSW effect on the expectations for the solar neutrino experiments in the maximal mixing scenario suggested by the atmospheric neutrino data. A direct numerical calculation of matter induced effects in the Sun shows that the naive vacuum predictions are left completely undisturbed in the particular case of maximal mixing, so that the MSW effect turns out to be unobservable. We give a qualitative explanation of this result.

To be published in Physics Letters B

¹E-mail:P.F.Harrison@QMW.AC.UK

²E-mail:D.Perkins1@OX.AC.UK

³E-mail:W.G.Scott@RL.AC.UK

There is no doubt that the famous Mikheyev-Smirnov-Wolfenstein (MSW) mechanism [1] [2] [3] continues to provide an elegant and viable explanation for the existing solar neutrino data [5] [4] [6] [7]. The preferred MSW fit requires one neutrino mass-squared difference $\sim 10^{-5} \text{ eV}^2$ and one small mixing angle $\sim 10^{-2}$ radians. On the other hand large mixing, and in particular maximal mixing [8] is not completely ruled out by the existing solar data and is in fact actively suggested by independent data relating to atmospheric neutrinos [9] [10] [11] [12]. The atmospheric neutrino data require a larger neutrino mass-squared difference $\sim 10^{-2} \text{ eV}^2$. In this paper we focus attention on the maximal mixing scenario [13] [14] suggested by the atmospheric data and proceed to investigate the possible influence of the MSW effect on the expectations for the solar neutrino experiments in that case. Our main results are based on a direct numerical calculation of matter induced effects in the Sun. We find that, in the maximal mixing scenario, matter induced effects turn out to be essentially unobservable, with the naive vacuum predictions left completely undisturbed, in the specific case of maximal mixing.

The MSW effect has its origin in the interaction of the solar neutrinos with the matter in the Sun. In particular in the presence of matter the neutrino mass matrix is modified by the forward scattering of electron-neutrinos from electrons via the weak charged current. In a weak basis which diagonalises the mass matrix of the charged leptons, the 3×3 vacuum propagation matrix $m^2/2E$ is replaced by a matter propagation matrix $m^2/2E + \text{diag}(\sqrt{2}GN_e, 0, 0)$, where $mm^\dagger \equiv m^2$ is the hermitian-square of the vacuum neutrino mass matrix, E is the neutrino energy, G is the Fermi constant, and N_e is the (position dependent) number density of electrons in the Sun.

We calculate the MSW effect numerically for arbitrary 3×3 vacuum mixing. To specify the vacuum mixing we take over the standard parameterisation [15] of the quark mixing matrix, so that, for example, threefold maximal mixing [13] is reproduced by setting $\theta_{12} = \theta_{23} = \pi/4$, $\theta_{13} = \sin^{-1}(1/\sqrt{3})$ and $\delta = \pi/2$. For given values of the input mixing parameters, we first construct a vacuum neutrino mass matrix (in the above basis) as a function of the two independent neutrino mass-squared differences Δm^2 and $\Delta m'^2$ ($\Delta m^2 \geq \Delta m'^2$ [13]). To account for matter effects we divide the propagation path longitudinally into thin slices of (variable) thickness Δ . For a given slice we calculate the matrix of transition amplitudes just as in the vacuum case ($A = \exp(-im^2\Delta/2E)$), but using the matter propagation matrix calculated assuming a constant density over the slice. The overall matrix of transition amplitudes is given by the ordered product of those for the individual slices, and the final electron-neutrino survival probability $P(e \rightarrow e)$ is averaged over neutrino energies for comparison with experiment.

Our calculation is ‘exact’ (at least in the limit $\Delta \rightarrow 0$) in the sense that it does not rely on any particular physical approximation relating to the MSW effect

itself (eg. ‘adiabatic approximation’ etc.). In practice, for the results presented below, we consider only radially directed propagation paths starting from the center of the Sun (the detailed production profile is unimportant here) and we average over a uniform distribution of neutrino energies with a width of $\pm 25\%$ [13]. The number density of electrons in the Sun as a function of radius R is parameterised [16] by $N_e = N_A \exp(5.50 - \sqrt{(10.54R/R_\odot)^2 + 0.89^2})$, where $N_A = 6.02 \times 10^{23} \text{ cm}^{-3}$ and $R_\odot = 0.7 \times 10^6 \text{ km}$ is the solar radius. For given Δm^2 and $\Delta m'^2$, typically ~ 1000 propagation slices and ~ 2500 energy samplings proved sufficient to produce a robust result. High precision (128-bit) arithmetic was found to be necessary for carrying out the matrix manipulations.

We first present results for the case of 2×2 mixing, ie. for a simplified scenario in which one of the three generations is completely decoupled in the mixing matrix and may in effect be forgotten. In the 2×2 case the mixing is completely specified by a single mass-squared difference Δm^2 , and by a single mixing angle θ . Figure 1 shows our results for 2×2 mixing. Figure 1a is for vacuum mixing only, ie. with matter induced effects neglected, and Figure 1b shows our results with matter induced effects taken into account. We plot the expected electron survival probability $P(e \rightarrow e)$ for solar neutrinos, as measured on Earth, as a function of $\Delta m^2/E$, for various values of $\sin \theta$ as indicated. For $\Delta m^2/E \lesssim 10^{-12} \text{ eV}^2/\text{MeV}$, the oscillation length is longer than the distance from the Sun to the Earth and $P(e \rightarrow e) = 1$. In the case of vacuum mixing the biggest suppression (a factor of $1/2$) occurs in the case of twofold maximal mixing ($\sin \theta \equiv 1/\sqrt{2}$). With matter effects included, for $\sin \theta < 1/\sqrt{2}$ (eg. for $\sin \theta = 0.5$, see Figure 1b) we reproduce the familiar MSW ‘bathtub’ [17] suppression, extending over the range $\Delta m^2/E = 10^{-8} - 10^{-5} \text{ eV}^2/\text{MeV}$. For $\sin \theta > 1/\sqrt{2}$ (eg. for $\sin \theta = 0.9$, see Figure 1b) we have an inverted bathtub, ie. an MSW enhancement. The MSW enhancement occurs when the *lighter* charged lepton, the electron, couples preferentially to the *heavier* neutrino (the rows and columns of the mixing matrix are ordered in increasing mass). In the case of twofold maximal mixing there is neither a suppression nor an enhancement. The solid curve in Figure 1b is identical to the corresponding curve in Figure 1a. We conclude that in the 2×2 context the MSW effect is unobservable in the particular case of maximal mixing.

Our results for 3×3 mixing are shown in Figure 2. For the 3×3 case we compute the survival probability $P(e \rightarrow e)$ as a function of the smaller independent mass-squared difference $\Delta m'^2$, with the larger mass-squared difference Δm^2 fixed by the atmospheric neutrino data ($\Delta m^2 \equiv 10^{-2} \text{ eV}^2$). The MSW effect is now governed by $|U_{2e}|$, the magnitude of the element of the mixing matrix linking the electron with the second lightest neutrino mass eigenstate. In the standard parameterisation [15] $U_{2e} = \cos \theta_{13} \sin \theta_{12}$. For the results presented in Figure 2 we vary $|U_{2e}|$ by varying θ_{12} ,

keeping θ_{23} , θ_{13} and δ fixed. For $\Delta m'^2/E \lesssim 10^{-12}$ eV²/MeV we have $P(e \rightarrow e) = 5/9$. Figure 2a is for vacuum mixing only and Figure 2b shows our results with matter effects included. In the case of vacuum mixing the biggest suppression (a factor of 1/3 for 3×3 mixing) occurs in the case of threefold maximal mixing. With matter effects included, the MSW effect leads to a suppression or an enhancement, in general, depending on the value of θ_{12} , as shown by the broken curves in Figure 2b. The MSW effect has no influence at all, however, in the particular case of threefold maximal mixing (cf. the solid curves in Figure 2b and Figure 2a) mirroring exactly our results for the 2×2 case above.

For completeness it should be said that if the larger mass-squared difference Δm^2 were *not* constrained by the atmospheric data *and* if it fell in the appropriate range viz. $\Delta m^2 = 10^{-8} - 10^{-5}$ eV², then the MSW effect would become observable in the case of threefold maximal mixing. The effect, however (assuming $\Delta m^2 \gg \Delta m'^2$), is simply to suppress $P(e \rightarrow e)$ by a factor of 1/3 (instead of 5/9) over the range of the bathtub, as shown in Figure 3, so that again the observable suppression factors are in general identical to the case of vacuum mixing.

With a view to obtaining a better understanding of the evident ‘special case’ status of maximal mixing with respect to the MSW effect, we return, for simplicity, to reconsider the case of 2×2 mixing, as a function of $\Delta m^2/E$, for an arbitrary mixing angle θ , as before. The effective Hamiltonian for the MSW system is just the matter propagation matrix above, which in the 2×2 case $\nu_e - \nu_\mu$ (say), may be written:

$$\begin{pmatrix} -(\Delta m^2/2E) \cos 2\theta + GN_e/\sqrt{2} & (\Delta m^2/2E) \sin 2\theta \\ (\Delta m^2/2E) \sin 2\theta & (\Delta m^2/2E) \cos 2\theta - GN_e/\sqrt{2} \end{pmatrix}. \quad (1)$$

In vacuum, in the small θ limit, ν_μ is the heavy mass eigenstate. In the high density limit ν_e is the heavy mass eigenstate. The familiar near-total MSW suppression of the ν_e flux for small mixing angles occurs when the matter density profile in the Sun provides a smooth matching from the ν_e state at the point of production, to a near- ν_μ state outside the Sun.

We exploit an analogy between the $\nu_e - \nu_\mu$ system in the presence of a variable matter density, and the behaviour of a spin-1/2 dipole at rest in a time-dependent uniform magnetic field. Suppose that the dipole has a negative magnetic moment $-\mu$. Suppose further that the magnetic field \mathbf{B} seen by the dipole may be decomposed as the vector sum of a constant (ie. time independent) ‘intrinsic’ field \mathbf{B}^0 and a variable (ie. time dependent) ‘external’ field \mathbf{B}_e . If the external field \mathbf{B}_e is directed along the quantisation axis (the z -axis) while the intrinsic field \mathbf{B}^0 makes an angle 2θ with respect to the negative z -axis and is contained in the zx -plane, then the Hamiltonian

for the dipole may be written:

$$\begin{pmatrix} -\mu B^0 \cos 2\theta + \mu B_e & \mu B^0 \sin 2\theta \\ \mu B^0 \sin 2\theta & \mu B^0 \cos 2\theta - \mu B_e \end{pmatrix}. \quad (2)$$

Comparing Eqs. 1 and 2 we see that, with the correspondence $\mu B^0 \leftrightarrow \Delta m^2/(2E)$ and $\mu B_e \leftrightarrow GN_e/\sqrt{2}$, the dipole and the MSW system have the same Hamiltonian. The utility of the analogy lies in the fact that the behaviour of the dipole is readily understood, since the spin vector \mathbf{S} for the dipole satisfies a well known classical equation of motion ($\dot{\mathbf{S}} = -2\mu\mathbf{S} \wedge \mathbf{B}$). The dipole simply precesses around the instantaneous magnetic field \mathbf{B} , with instantaneous angular frequency $2\mu B$.

The small angle MSW effect may now be viewed as the adiabatic reversal of the spin of the dipole, in response to the slow reversal of the field \mathbf{B} , as the external field \mathbf{B}_e decreases to zero. This is illustrated in Figure 4. The resonance condition is satisfied when \mathbf{B} is directed horizontally along the x -axis, and the mixing becomes momentarily maximal. If the vacuum mixing is anyway maximal the intrinsic field \mathbf{B}^0 is directed entirely horizontally along the x -axis and no such reversal can occur. The inverted bathtub seen for large mixing angles corresponds to the case that \mathbf{B}^0 points upwards. In the maximal mixing case, the dipole simply follows \mathbf{B} smoothly from the vertical to the horizontal and remains horizontal, yielding 50% spin-up (ν_e) and 50% spin-down (ν_μ), just as for maximal mixing in vacuum. The difference is that in the matter case the residual oscillations are small, while in the vacuum case the dipole precesses around the x -axis, corresponding to maximal (100%) oscillations. It is only because these oscillations are unresolved that the matter and the vacuum predictions turn out to be indistinguishable. Presumably the behaviour in the 3×3 case has some closely related explanation, but we have not attempted to consider the 3×3 case in the equivalent level of detail.

To summarise, a direct numerical calculation shows that the MSW effect is unobservable in the particular case of maximal mixing. The naive vacuum predictions are left completely undisturbed in that case. This result is valid for 2×2 mixing for any value of Δm^2 , and for 3×3 mixing for any value of $\Delta m'^2$, with $\Delta m^2 \sim 10^{-2} \text{eV}^2$, fixed by the atmospheric neutrino data. Exploiting the analogy between the MSW effect in 2×2 mixing and the behaviour of a spin-1/2 dipole in a time-dependent magnetic field, we have given a qualitative explanation of this result. It is true nonetheless that the small angle MSW solution, with appropriate choices for the parameters, gives an excellent fit to the existing solar data, and is currently (perhaps not unnaturally therefore) widely accepted as *the* solution to the solar neutrino problem. While our results do not in any way undermine the validity of the MSW solution, they do serve to draw attention to an interesting and significant exception, where the MSW mechanism cannot be invoked. The MSW and maximal mixing scenarios as solutions to the

solar neutrino problem are, in a very definite and real sense, to be seen as mutually exclusive alternatives.

Acknowledgement

It is a pleasure to thank Roger Phillips for a number of useful discussions.

References

- [1] L. Wolfenstein, Phys. Rev. D17 (1978) 2369; D20 (1979) 2634.
- [2] S. P. Mikheyev and A. Yu. Smirnov, Il Nuovo Cimento 9C (1986) 17.
- [3] V. Barger et al., Phys. Rev. D22 (1980) 2718.
H. A. Bethe, Phys. Rev. Lett. 56 (1986) 1305.
S. P. Rosen and J. M. Gelb, Phys. Rev. D34 (1986) 969.
S. P. Rosen and W. Kwong, UTAPHY-HEP-13 (1995).
- [4] K. S. Hirata et al., Phys. Rev. Lett. 65 (1990) 1297; 66 (1991) 9;
Phys. Rev. D44 (1992) 146.
- [5] B. T. Cleveland et al., Nucl. Phys. B (Proc. Suppl.) 38 (1995) 47.
- [6] A. I. Abazov et al., Phys. Rev. Lett. 67 (1991) 3332.
J. N. Abdurashitov et al., Phys. Lett. B 328 (1994) 234.
- [7] P. Anselmann et al., Phys. Lett. B285 (1992) 376; B314 (1993) 445;
B342 (1995) 440; B357 (1995) 237.
- [8] S. Nussinov, Phys. Lett. 63B (1976) 201.
L. Wolfenstein, Phys. Rev D18 (1978) 958.
N. Cabibbo, Phys. Lett. B72 (1978) 333.
P. F. Harrison and W. G. Scott, Phys. Lett. B333 (1994) 471.
- [9] K. S. Hirata et al., Phys. Lett. B205 (1988) 416; B280 (1992) 146.
Y. Fukada et al. Phys. Lett. B335 (1994) 237.
- [10] R. Becky-Szandy et al., Phys. Rev. D46 (1992) 3720.
D. Casper et al., Phys. Rev. Lett. 66 (1992) 2561.
- [11] P. J. Litchfield, Proceedings of the XV Workshop on Weak Interactions
and Neutrinos, Talloires, France (1995).
- [12] S. Ahlen et al., Phys. Lett. B 357 (1995) 481.

- [13] P.F. Harrison, D. H. Perkins and W. G. Scott, Phys. Lett. B 349 (1995) 137.
- [14] C. Giunti, C. W. Kim and J. D. Kim, Phys. Lett. B352 (1995) 357.
- [15] Particle Data Group, Particle Physics Booklet (1994).
- [16] J. N. Bahcall, Neutrino Astrophysics. Cambridge University Press, New York (1989).
- [17] R. J. N. Phillips, Proceedings of the International meeting on Solar Neutrinos, Goa, India. RAL-94-017.

Figure Captions

Figure 1. The expected electron-neutrino survival probability $P(e \rightarrow e)$, for solar neutrinos, as measured on Earth, for the case of 2×2 mixing. The survival probability is plotted as a function of $\Delta m^2/E$ for various values of $\sin \theta$, as indicated, for a) vacuum mixing and b) accounting for matter induced effects in the Sun. In the particular case of maximal mixing (solid curves) the vacuum and matter curves are indistinguishable.

Figure 2. The expected electron-neutrino survival probability $P(e \rightarrow e)$, for solar neutrinos, as measured on Earth, for the case of 3×3 mixing. The survival probability is plotted as a function of $\Delta m'^2/E$ (with $\Delta m^2 \equiv 10^{-2} \text{ eV}^2$) for various values of θ_{12} , as indicated, for a) vacuum mixing and b) accounting for matter induced effects in the Sun. In the particular case of threefold maximal mixing (solid curves) the vacuum and matter curves are indistinguishable.

Figure 3. If Δm^2 were not constrained by the atmospheric data, the MSW effect would become observable in threefold maximal mixing for $\Delta m^2 = 10^{-8} - 10^{-5} \text{ eV}^2$, as shown (assuming $\Delta m'^2 \ll \Delta m^2$). The suppression factor is $1/3$ (instead of $5/9$) over the range of the ‘bathtub’, however, so that the observable suppression factors are anyway identical to those for the vacuum case.

Figure 4. The near-total MSW suppression of the ν_e flux for small mixing angles is analogous to the adiabatic reversal of a spin-1/2 dipole in the time dependent magnetic field illustrated. As the ‘external’ field \mathbf{B}_e decreases to zero for fixed ‘intrinsic’ field \mathbf{B}^0 as shown, the resultant field \mathbf{B} seen by the dipole reverses. In the case of maximal mixing the intrinsic field \mathbf{B}^0 is directed entirely along the x -axis and no such reversal occurs.

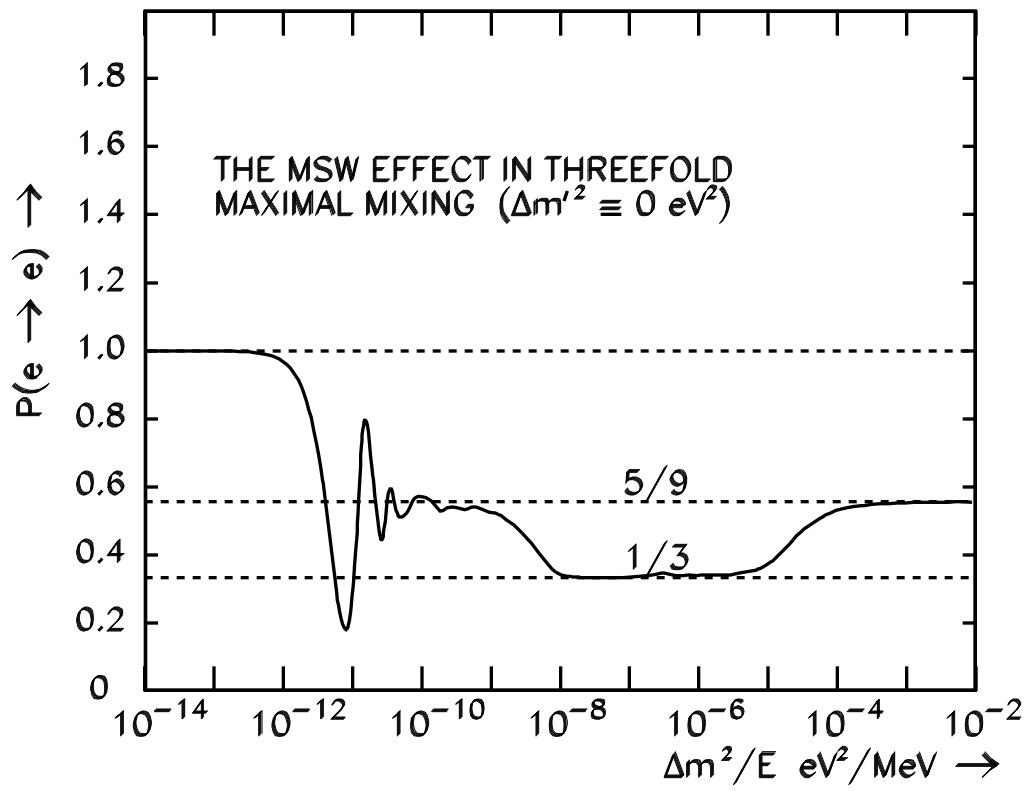


Figure 3

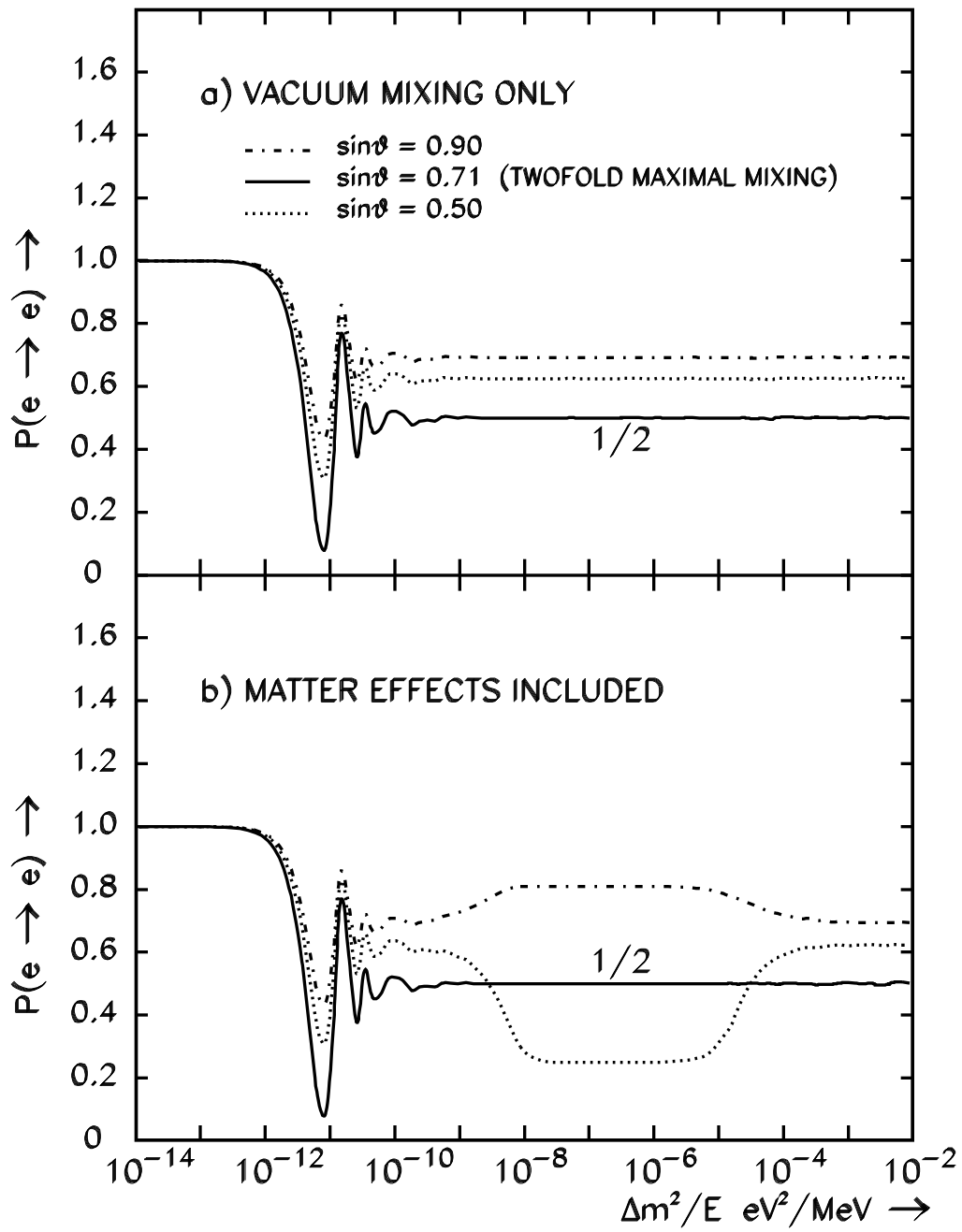


Figure 1

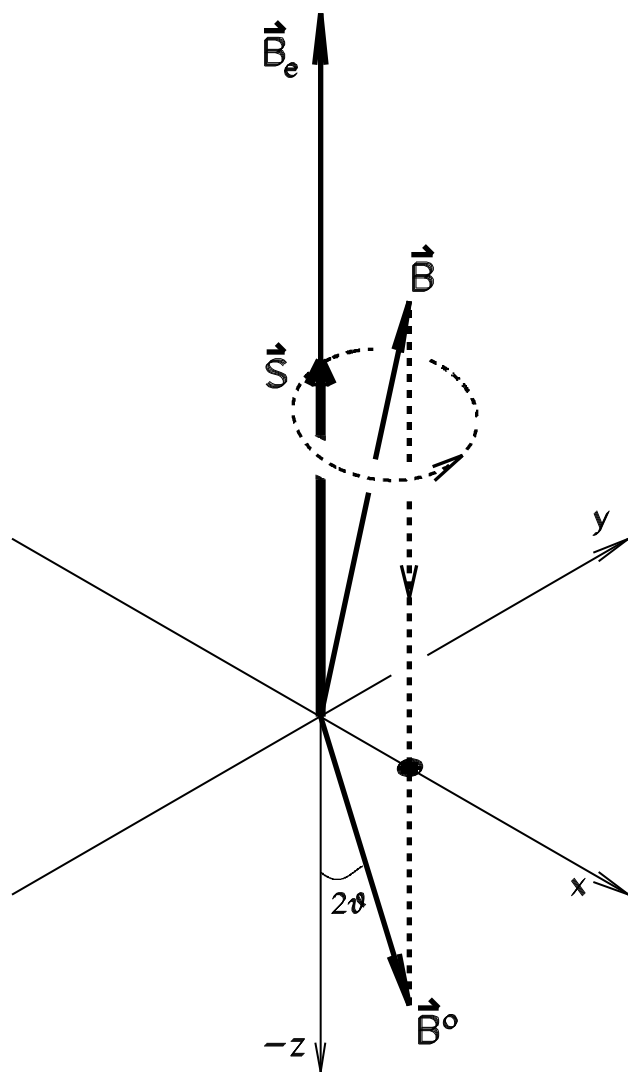


Figure 4

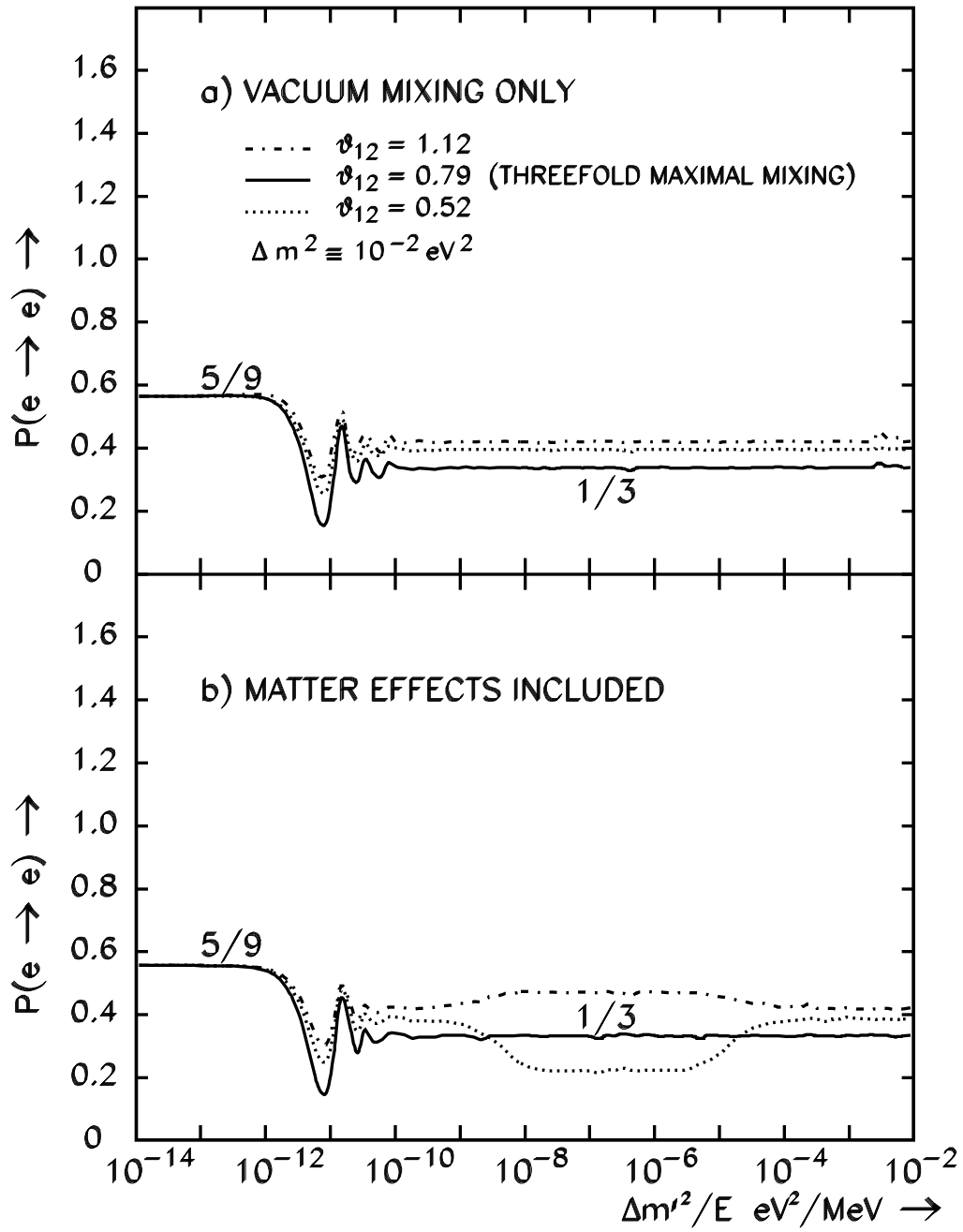


Figure 2